



Queensland University of Technology
Brisbane Australia

This is the author's version of a work that was submitted/accepted for publication in the following source:

Frost, Ray L., Xi, Yunfei, & Palmer, Sara J. (2012) Raman spectroscopy of the multianion mineral gartrellite-PbCu(Fe³⁺,Cu)(AsO₄)₂(OH,H₂O)₂. *Spectrochimica Acta, Part A : Molecular and Biomolecular Spectroscopy*, 89, pp. 93-98.

This file was downloaded from: <http://eprints.qut.edu.au/48772/>

© Copyright 2012 Elsevier

This is the author's version of a work that was accepted for publication in <Spectrochimica Acta, Part A : Molecular and Biomolecular Spectroscopy>. Changes resulting from the publishing process, such as peer review, editing, corrections, structural formatting, and other quality control mechanisms may not be reflected in this document. Changes may have been made to this work since it was submitted for publication. A definitive version was subsequently published in Spectrochimica Acta, Part A : Molecular and Biomolecular Spectroscopy, [VOL 89, (2012)] DOI: 10.1016/j.saa.2011.12.034

Notice: *Changes introduced as a result of publishing processes such as copy-editing and formatting may not be reflected in this document. For a definitive version of this work, please refer to the published source:*

<http://dx.doi.org/10.1016/j.saa.2011.12.034>

1 **Raman spectroscopy of the multianion mineral gartrellite**



3
4 **Ray L. Frost, • Yunfei Xi, Sara J. Palmer**

5
6 Chemistry Discipline, Faculty of Science and Technology, Queensland University of
7 Technology, GPO Box 2434, Brisbane Queensland 4001, Australia.

8
9 **Abstract**

10 The multianion mineral gartrellite $\text{PbCu}(\text{Fe}^{3+}, \text{Cu})(\text{AsO}_4)_2(\text{OH}, \text{H}_2\text{O})_2$ has been studied by a
11 combination of Raman and infrared spectroscopy. The vibrational spectra of two gartrellite
12 samples from Durango and Ashburton Downs were compared. Gartrellite is one of the
13 tsumcorite mineral group based upon arsenate and sulphate anions. Crystal symmetry is
14 either triclinic in the case of an ordered occupation of two cationic sites, triclinic due to
15 ordering of the H bonds in the case of species with 2 water molecules per formula unit, or
16 monoclinic in the other cases. Characteristic Raman spectra of the minerals enable the
17 assignment of the bands to specific vibrational modes. These spectra are related to the
18 structure of gartrellite. The position of the hydroxyl and water stretching vibrations are
19 related to the strength of the hydrogen bond formed between the OH unit and the AsO_4 anion.

20
21 **Keywords:** Raman spectroscopy, gartrellite, tsumcorite, thometzekite, arsenate, sulphate

22
23
24

• Author to whom correspondence should be addressed (r.frost@qut.edu.au)

25 Introduction

26 The mineral gartrellite $\text{PbCu}(\text{Fe}^{3+}, \text{Cu})(\text{AsO}_4)_2(\text{OH}, \text{H}_2\text{O})_2$ is triclinic with space group: $P1$, a
27 $= 5.431\text{--}5.460$, $b = 5.628\text{--}5.653$, $c = 7.565\text{--}7.589$, $\alpha = 67.52\text{--}67.77$, $\beta = 69.27\text{--}69.57$, $\gamma =$
28 $70.04\text{--}70.31$ and $Z = 1$ [1]. Gartrellite [2] is a rare mineral found in the oxidised mineralised
29 shear zone cutting graywackes and shales as in the Anticline prospect, Australia and on fine-
30 grained quartz-spessartine rocks at Broken Hill, Australia. The mineral is associated with
31 hidalgoite–beudantite, quartz, spessartine (Broken Hill, Australia); mimetite, duftite,
32 beudantite, bayldonite and quartz (Tsumeb, Namibia) [3].

33

34 Gartrellite is a member of the tsumcorite mineral group. The tsumcorite group of minerals are
35 a mineral group based upon monoclinic and triclinic arsenates, phosphates, vanadates and
36 sulphates of the general formulae $(\text{M1})(\text{M2})_2(\text{XO}_4)_2(\text{OH}, \text{H}_2\text{O})_2$ where M1 is Pb, Ca or Na,
37 M2 is Cu, Zn, Fe^{3+} , Co or Mn and X is As, P, V or S. The minerals gartrellite
38 $\text{Pb}[(\text{Cu}, \text{Zn})(\text{Fe}^{3+}, \text{Zn}, \text{Cu})](\text{AsO}_4)(\text{OH}, \text{H}_2\text{O})_2$, helmutwinklerite $\text{Pb}(\text{Zn}, \text{Cu})_2(\text{AsO}_4)_2 \cdot 2\text{H}_2\text{O}$ and
39 thometzekite [4] are triclinic. The minerals ferrilotharmeyerite [5]
40 $\text{Ca}(\text{Fe}^{3+}, \text{Zn})_2(\text{AsO}_4)_2(\text{OH}, \text{H}_2\text{O})_2$, lotharmeyerite $\text{Ca}(\text{Mn}^{3+}, \text{Zn})_2(\text{AsO}_4)_2(\text{OH}, \text{H}_2\text{O})_2$, mawbyite
41 [6] $\text{Pb}(\text{Fe}^{3+}, \text{Zn})_2(\text{AsO}_4)_2(\text{OH}, \text{H}_2\text{O})_2$, mounanaite $\text{Pb}(\text{Fe}^{3+})_2(\text{VO}_4)_2(\text{OH})_2$, natrochalcite [7]
42 $\text{NaCu}_2(\text{SO}_4)_2(\text{OH}, \text{H}_2\text{O})_2$ and tsumcorite [8] $\text{Pb}(\text{Zn}, \text{Fe}^{3+})_2(\text{AsO}_4)_2(\text{OH}, \text{H}_2\text{O})$ are monoclinic.
43 [8].

44

45 There are some problems associated with writing the mineral formula, in that the formula
46 may change as a function of the degree of solid solution formation and the amount of
47 isomorphic substitution. Both anion and cation substitution may occur. Sulphate, phosphate
48 and carbonate may replace arsenate. For example, it is quite comprehensible that a formula
49 such as $\text{PbCu}(\text{Fe}^{3+}, \text{Cu})(\text{AsO}_4)_2(\text{OH}, \text{H}_2\text{O})_2$ is possible. Variation in mineral composition is
50 expected for gartrellites from different origins. The formula may be written as
51 $\text{Pb}[(\text{Cu}, \text{Fe}^{2+})(\text{Fe}^{3+}, \text{Zn}, \text{Cu})](\text{AsO}_4)(\text{CO}_3, \text{H}_2\text{O})_2$. For example, the gartrellite found at
52 Ashburton Downs, Western Australia has a calculated formula of
53 $\text{PbCu}_{1.5}\text{Fe}^{2+}_{0.5}\text{As}_{1.5}(\text{SO}_4)_{0.5}(\text{CO}_3)_{0.5}(\text{H}_2\text{O})_{0.2}$. Of course, Raman spectroscopy will readily
54 determine the presence of carbonate in the mineral. The presence or absence of two moles of
55 water is the determining factor as to whether the mineral is triclinic or not.

56 Crystal symmetry is either triclinic in the case of an ordered occupation of two cationic sites
57 (triclinic due to ordering of the H bonds in the case of species with 2 water molecules per
58 formula unit) or monoclinic in the other cases. Crystals of ferrilotharmeyerite, tsumcorite,
59 thometzekite (sulfatian), and mounanaite have monoclinic symmetry and space group C2/m.
60 The triclinic members of the tsumcorite group are gartrellite, zincian gartrellite,
61 phosphogartrellite, helmutwinklerite, and probably (sulphate-free) thometzekite; the space
62 group is P1 with a pronounced monoclinic C-centered pseudocell. The triclinic distortion is
63 caused by an ordered arrangement of Fe[6]O₆ octahedra and tetragonal bi-pyramidal
64 Cu[4+2]O₆ polyhedra [5].

65 Raman spectroscopy has proven very useful for the study of minerals [9-15]. Indeed Raman
66 spectroscopy has proven most useful for the study of diagenetically related minerals as often
67 occurs with minerals containing sulphate, arsenate and/or phosphate groups. Raman
68 spectroscopy is especially useful when the minerals are X-ray non-diffracting or poorly
69 diffracting and very useful for the study of amorphous and colloidal minerals. This paper is a
70 part of systematic studies of vibrational spectra of minerals of secondary origin in the oxide
71 supergene zone. In this work we attribute bands at various wavenumbers to vibrational modes
72 of gartrellite using Raman spectroscopy and relate the spectra to the structure of the mineral.

73 **Experimental**

74 **Minerals**

75 Gartrellite was obtained from Museum Victoria with sample number m39987 and originated
76 from the Anticline Deposit, Ashburton Downs, WA. A second sample of the mineral
77 gartrellite was supplied by The Mineralogical Research Company. The sample originated
78 from the Ojuela Mine, Mapini, Durango, Mexico. Details of the gartrellite mineral have been
79 published (page 207) [3].

80 **Raman spectroscopy**

81 Crystals of gartrellite were placed on a polished metal surface on the stage of an Olympus
82 BHSM microscope, which is equipped with 10x, 20x, and 50x objectives. The microscope is
83 part of a Renishaw 1000 Raman microscope system, which also includes a monochromator, a
84 filter system and a CCD detector (1024 pixels). The Raman spectra were excited by a
85 Spectra-Physics model 127 He-Ne laser producing highly polarised light at 633 nm and
86 collected at a nominal resolution of 2 cm⁻¹ and a precision of ± 1 cm⁻¹ in the range between

87 100 and 4000 cm^{-1} . Repeated acquisition on the crystals using the highest magnification (50x)
88 was accumulated to improve the signal to noise ratio in the spectra. Spectra were calibrated
89 using the 520.5 cm^{-1} line of a silicon wafer.

90 **Infrared spectroscopy**

91 Infrared spectra were obtained using a Nicolet Nexus 870 FTIR spectrometer with a smart
92 endurance single bounce diamond ATR cell. Spectra over the 4000–525 cm^{-1} range were
93 obtained by the co-addition of 128 scans with a resolution of 4 cm^{-1} and a mirror velocity of
94 0.6329 cm/s . Spectra were co-added to improve the signal to noise ratio.

95 Band component analysis was undertaken using the Jandel ‘Peakfit’ (Erkrath,
96 Germany) software package which enabled the type of fitting function to be selected and
97 allowed specific parameters to be fixed or varied accordingly. Band fitting was done using a
98 Lorentz-Gauss cross-product function with the minimum number of component bands used
99 for the fitting process. The Lorentz-Gauss ratio was maintained at values greater than 0.7 and
100 fitting was undertaken until reproducible results were obtained with squared correlations (r^2)
101 greater than 0.995. Band fitting of the spectra is quite reliable providing there is some band
102 separation or changes in the spectral profile.

103 **Results and discussion**

104 **Arsenate vibrations**

105 According to Myneni *et al.* [16, 17] and Nakamoto [18], $(\text{AsO}_4)^{3-}$ is a tetrahedral unit,
106 which exhibits four fundamental vibrations: the Raman active ν_1 symmetric stretching
107 vibration (A_1) 818 cm^{-1} ; the Raman active doubly degenerate ν_2 symmetric bending vibration
108 (E) 350 cm^{-1} , the infrared and Raman active triply degenerate ν_3 antisymmetric stretching
109 vibration (F_2) 786 cm^{-1} , and the infrared and Raman active triply degenerate ν_4 bending
110 vibration (F_2) 405 cm^{-1} . Protonation, metal complexation, and/or adsorption on a mineral
111 surface will cause the change in $(\text{AsO}_4)^{3-}$ symmetry from T_d to lower symmetries, such as
112 C_{3v} , C_{2v} or even C_1 . This loss of degeneracy causes splitting of degenerate vibrations of
113 $(\text{AsO}_4)^{3-}$ and the shifting of the As-OH stretching vibrations to different wavenumbers.
114 Sulphates as with other oxyanions lend themselves to analysis by Raman spectroscopy [19].
115 In aqueous systems, the sulphate anion is of T_d symmetry and is characterised by Raman
116 bands at 981 cm^{-1} (ν_1), 451 cm^{-1} (ν_2), 1104 cm^{-1} (ν_3) and 613 cm^{-1} (ν_4). Reduction in

117 symmetry in the crystal structure of sulphates, such as in a number of minerals, will cause the
118 splitting of these vibrational modes.

119 Such chemical interactions reduce $(\text{AsO}_4)^{3-}$ tetrahedral symmetry, as mentioned
120 above, to either C_{3v}/C_3 (corner-sharing), C_{2v}/C_2 (edge-sharing, bidentate binuclear), or C_1/C_s
121 (corner-sharing, edge-sharing, bidentate binuclear, multidentate) [16, 17]. In association with
122 $(\text{AsO}_4)^{3-}$ symmetry and coordination changes, the A_1 band may shift to different
123 wavenumbers and the doubly degenerate E and triply degenerate F modes may give rise to
124 several new A_1 , B_1 , and/or E vibrations [16, 17]. In the absence of symmetry deviations,
125 $(\text{AsO}_3\text{OH})^{2-}$ in C_{3v} symmetry exhibit the ν_s As-OH and ν_{as} and ν_s $(\text{AsO}_3\text{OH})^{2-}$ vibrations
126 together with corresponding the δ As-OH in-plane bending vibration, δ As-OH out-of-plane
127 bending vibration, ν_s $(\text{AsO}_3\text{OH})^{2-}$ stretching vibration and δ_{as} $(\text{AsO}_3\text{OH})^{2-}$ bending vibration
128 [20-22]. Keller [20] observed the following infrared bands in $\text{Na}_2(\text{AsO}_3\text{OH})\cdot 7\text{H}_2\text{O}$ 450 and
129 assigned bands at 360 cm^{-1} to δ_{as} (ν_4) $(\text{AsO}_3\text{OH})^{2-}$ bend (E), 580 cm^{-1} to the δ As-OH out-of-
130 plane bend, 715 cm^{-1} to the ν As-OH stretch (A_1), 830 cm^{-1} to the ν_{as} $(\text{AsO}_3\text{OH})^{2-}$ stretch (E),
131 and 1165 cm^{-1} to the δ As-OH in plane bend. In the Raman spectrum of $\text{Na}_2(\text{AsO}_3\text{OH})\cdot 7\text{H}_2\text{O}$,
132 Vansant *et al.* [21] attributed Raman bands to the following vibrations 55, 94, 116 and 155
133 cm^{-1} to lattice modes, 210 cm^{-1} to ν (OH...O) stretch, 315 cm^{-1} to $(\text{AsO}_3\text{OH})^{2-}$ rocking, 338
134 cm^{-1} to the δ_s $(\text{AsO}_3)^{2-}$ bend, 381 cm^{-1} to the δ_{as} $(\text{AsO}_3\text{OH})^{2-}$ bend, 737 cm^{-1} to the ν_s As-OH
135 stretch (A_1), 866 cm^{-1} to the ν_{as} $(\text{AsO}_3\text{OH})^{2-}$ stretch (E).

136 **Raman and Infrared Spectroscopy**

137 The Raman spectrum of the Durango gartrellite in the 700 to 1000 cm^{-1} region is displayed in
138 Figure 1a. Five Raman bands are observed at 799 , 811 , 830 , 866 and 891 cm^{-1} . The last two
139 bands are assigned to the Raman active ν_1 symmetric stretching vibration (A_1). The first three
140 bands are assigned to the infrared and Raman active triply degenerate ν_3 antisymmetric
141 stretching vibration (F_2). The Raman spectrum of the Ashburton Downs gartrellite is
142 reported in Figure 1b. Raman bands are observed at 754 , 810 , 842 and 868 cm^{-1} . The
143 gartrellite sample from Ashburton Downs displays additional bands at 995 , 1096 and 1158
144 cm^{-1} . These bands were not observed in the spectrum of the Durango gartrellite. The band at
145 995 cm^{-1} is assigned to the SO_4^{2-} symmetric stretching mode and the two bands at 1096 and
146 1158 cm^{-1} to the SO_4^{2-} antisymmetric stretching mode.

147 The infrared spectrum of Durango gartrellite is shown in Figure 2. The infrared spectrum
148 consists of a broad profile which may be resolved into component bands at 723, 782, 804,
149 826, 842 and 897 cm^{-1} . Other low intensity bands are found on the low wavenumber side at
150 579, 587 and 629 cm^{-1} ; and on the high wavenumber side at 1002, 1023, 1076 and 1105 cm^{-1} .
151 One probable assignment, in harmony with the Raman data is that the bands at 723, 782 and
152 804 cm^{-1} are due to the ν_3 antisymmetric stretching vibrations and the bands at 842 and 897
153 cm^{-1} are due to the ν_1 symmetric stretching vibration. The low intensity bands between 1000
154 and 1200 cm^{-1} are attributed to the sulphate stretching vibrations.

155 The Raman spectra of the Durango and Ashburton Downs gartrellite in the 100 to 600 cm^{-1}
156 region are shown in Figures 3a and 3b respectively. This spectral region is where the
157 arsenate and sulphate bands overlap. This makes the exact assignment of bands difficult.
158 Raman bands for the Durango gartrellite are observed at 421, 454, 487 and 507 cm^{-1} and for
159 the Ashburton Downs gartrellite at 435, 473 and 498 cm^{-1} . These may be ascribed to the
160 AsO_4^{3-} ν_4 bending modes. It is probable that the Raman bands at 554 cm^{-1} (Durango) and
161 558 cm^{-1} (Ashburton) are associated with SO_4^{3-} bending modes. The Raman bands at 313,
162 338 and 382 cm^{-1} (Durango) and 302, 328 and 355 cm^{-1} (Ashburton) are assigned to the
163 AsO_4^{3-} ν_2 bending modes. The Raman spectra in the 100 to 300 cm^{-1} region of the two
164 gartrellite samples are different. Intense Raman bands are observed at 180 cm^{-1} (Durango)
165 and 200 cm^{-1} (Ashburton) are thought to be associated with hydrogen bonding of OH units
166 and water units to the arsenate and sulphate anions. It is also expected that some bands are
167 associated with Pb or Cu oxygen stretching bands.

168 The Raman spectrum of the Durango and Ashburton Downs gartrellites in the hydroxyl
169 stretching region are displayed in Figures 4a and 4b, respectively. The spectrum consists of a
170 broad spectral profile centred upon 3090 cm^{-1} and a sharp band at 3514 cm^{-1} . This broad
171 spectral profile may be resolved into component bands at 2975, 3090 and 3240 cm^{-1} . These
172 latter three bands are assigned to water stretching bands, whilst the band at 3514 cm^{-1} is
173 assigned to the OH stretching vibration. Raman bands of the Ashburton Downs gartrellite are
174 observed at 2989 and 3217 cm^{-1} are assigned to the water stretching vibrations and the band
175 at 3396 cm^{-1} assigned to the OH stretching band. What is immediately obvious is that the
176 spectra in this spectral region are different. The position of the band assigned to the OH
177 stretching vibration is very different. This difference is attributed to the strength of the

178 hydrogen bond between the OH units and the arsenate anions. The hydrogen bonding in the
179 Ashburton Downs gartrellite is significantly stronger.

180

181 The infrared spectrum of the Durango gartrellite is reported in Figure 5. The infrared
182 spectrum strongly resembles the Raman spectrum. The spectrum consists of a broad spectral
183 profile and a sharp intense band at 3515 cm^{-1} . This sharp band is assigned to the OH
184 stretching vibration of the OH units. The broad spectral profile may be resolved into
185 component bands at 2525 , 2762 , 2956 and 3088 cm^{-1} . The position of these bands provides
186 evidence for strong hydrogen bonding between the water and the arsenate anions in the
187 mineral structure.

188

189 The Raman spectrum in the 1350 to 1850 cm^{-1} is displayed in Figure 6a. The concept of
190 strong hydrogen bonding in gartrellites is supported by the infrared spectrum in the 1250 to
191 1750 cm^{-1} region (Figure 6b) where an infrared band at 1677 cm^{-1} is found. This band is
192 attributed to water HOH bending modes. The bands at 1445 , 1523 and 1586 cm^{-1} are
193 attributed to OH deformation modes. The Raman equivalent water bending mode is not
194 observed in the Raman spectrum. This is not unexpected as water is a notoriously bad
195 Raman scatterer. The Raman spectrum suffers from a lack of signal to noise. The bands
196 observed are attributed to OH deformation modes.

197

198 **Conclusions**

199 A combination of Raman spectroscopy and infrared spectroscopy has been used to
200 characterise the arsenates and sulphates in the mineral gartrellite. Two gartrellite minerals
201 from different origins were studied. The spectra of the two mineral samples were different.
202 Extensive isomorphic substitution of sulphate for arsenate is observed. The fundamental
203 internal modes in the spectra are related to the structure of the minerals. Gartrellite shows a
204 much greater sulphate isomorphic substitution. The range of OH stretching wavenumbers
205 shows a range of hydrogen bond strengths based upon the range of calculated hydrogen bond
206 distances. High wavenumber bands around 3400 - 3500 cm^{-1} indicate the presence of OH
207 units in the gartrellite structure. Gartrellite minerals are characterised by typical spectra of

208 the AsO_4^{3-} units. The symmetric stretching modes are observed in the 840 to 880 cm^{-1}
209 region; while the antisymmetric stretching modes are observed in the 812 to 840 cm^{-1} region.
210 Some bands are observed around 765 cm^{-1} and are attributed to water librational modes. The
211 ν_4 bending modes are observed around 499 cm^{-1} and the ν_2 bending modes in the 300 to 360
212 cm^{-1} region. Multiple bands are observed in these regions indicating a loss of symmetry of
213 the AsO_4 unit.

214

215

216 **Acknowledgments**

217 The financial and infra-structure support of the Queensland University of Technology,
218 Chemistry discipline is gratefully acknowledged. The Australian Research Council (ARC) is
219 thanked for funding the instrumentation. Mr Dermot Henry of Museum Victoria is especially
220 thanked for the loan of the tsumcorite minerals.

221

222 **REFERENCES**

- 223 [1] W. Krause, K. Belendorff, H.J. Bernhardt, C. McCammon, H. Effenberger, W.
224 Mikenda, *European Journal of Mineralogy* 10 (1998) 179.
- 225 [2] J.L. Jambor, E.S. Grew, *American Mineralogist* 75 (1990) 931.
- 226 [3] J.W. Anthony, R.A. Bideaux, K.W. Bladh, M.C. Nichols, *Handbook of Mineralogy*
227 Vol.IV. Arsenates, phosphates, vanadates Mineral Data Publishing, . Mineral data Publishing,
228 Tucson, Arizona,, Tucson, Arizona, 2000.
- 229 [4] K. Schmetzer, B. Nuber, O. Medenbach, *Neues Jahrb. Mineral., Monatsh.* (1985) 446.
- 230 [5] W. Krause, K. Belendorff, H.J. Bernhardt, C. McCammon, H. Effenberger, W.
231 Mikenda, *European Journal of Mineralogy* 10 (1998) 179.
- 232 [6] Kharisun, M.R. Taylor, D.J.M. Bevan, A.D. Rae, A. Pring, *Mineralogical Magazine*
233 61 (1997) 685.
- 234 [7] I.M. Rumanova, G.F. Volodina, *Doklady Akad. Nauk S.S.S.R.* 123 (1958) 78.
- 235 [8] E. Tillmanns, W. Gebert, *Acta Crystallogr., Sect. B* 29 (1973) 2789.
- 236 [9] R.L. Frost, S. Bahfenne, *J. Raman Spectrosc.* 41 (2010) 207.
- 237 [10] R.L. Frost, S. Bahfenne, *J. Raman Spectrosc.* 41 (2010) 325.
- 238 [11] R.L. Frost, S. Bahfenne, J. Cejka, J. Sejkora, S.J. Palmer, R. Skoda, *J. Raman*
239 *Spectrosc.* 41 (2010) 690.
- 240 [12] R.L. Frost, S. Bahfenne, J. Cejka, J. Sejkora, J. Plasil, S.J. Palmer, *J. Raman*
241 *Spectrosc.* 41 (2010) 814.
- 242 [13] R.L. Frost, K.H. Bakon, S.J. Palmer, *J. Raman Spectrosc.* 41 (2010) 78.
- 243 [14] R.L. Frost, J. Cejka, J. Sejkora, J. Plasil, S. Bahfenne, S.J. Palmer, *J. Raman*
244 *Spectrosc.* 41 (2010) 571.
- 245 [15] R.L. Frost, J. Cejka, J. Sejkora, J. Plasil, S. Bahfenne, S.J. Palmer, *J. Raman*
246 *Spectrosc.* 41 (2010) 566.
- 247 [16] S.C.B. Myneni, S.J. Traina, G.A. Waychunas, T.J. Logan, *Geochim. Cosmochim.*
248 *Acta* 62 (1998) 3285.
- 249 [17] S.C.B. Myneni, S.J. Traina, G.A. Waychunas, T.J. Logan, *Geochim. Cosmochim.*
250 *Acta* 62 (1998) 3499.
- 251 [18] K. Nakamoto, *Infrared and Raman Spectra of Inorganic and Coordination*
252 *Compounds.*, Wiley New York 1986.
- 253 [19] R.L. Frost, P.A. Williams, W. Martens, P. Leverett, J.T. Klopogge, *American*
254 *Mineralogist* 89 (2004) 1130.

- 255 [20] P. Keller, Neues Jb. Miner. Mh. (1971) 491.
- 256 [21] F.K. Vansant, B.J.V.D. Veken, J. Mol. Struct. 15 (1973) 439.
- 257 [22] F.K. Vansant, B.J.V.D. Veken, H.O. Desseyn, J. Mol. Struct. (1973) 425.
- 258
- 259
- 260
- 261
- 262
- 263
- 264

265 **List of Figures**

266 **Figure 1 Raman spectra of gartrellite from (a) Durango (b) Ashburton Downs in the 700**
267 **to 1200 cm⁻¹ region.**

268 **Figure 2 Infrared spectrum of gartrellite from Durango in the 500 to 1200 cm⁻¹ region**

269 **Figure 3 Raman spectra of gartrellite from (a) Durango (b) Ashburton Downs in the 100**
270 **to 600 cm⁻¹ region.**

271 **Figure 4 Raman spectra of gartrellite from (a) Durango (b) Ashburton Downs in the**
272 **2500 to 3700 cm⁻¹ region.**

273 **Figure 5 Infrared spectrum of gartrellite from Durango in the 2200 to 3700 cm⁻¹ region**

274 **Figure 6a Raman spectrum of Durango gartrellite in the 1350 to 1850 cm⁻¹ region**

275 **Figure 6b Infrared spectrum of Durango gartrellite in the 1250 to 1800 cm⁻¹ region**

276

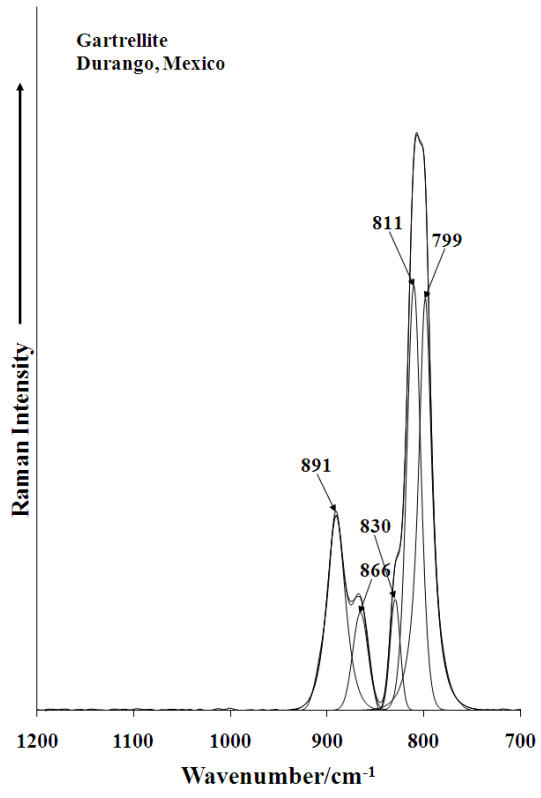


Figure 1a

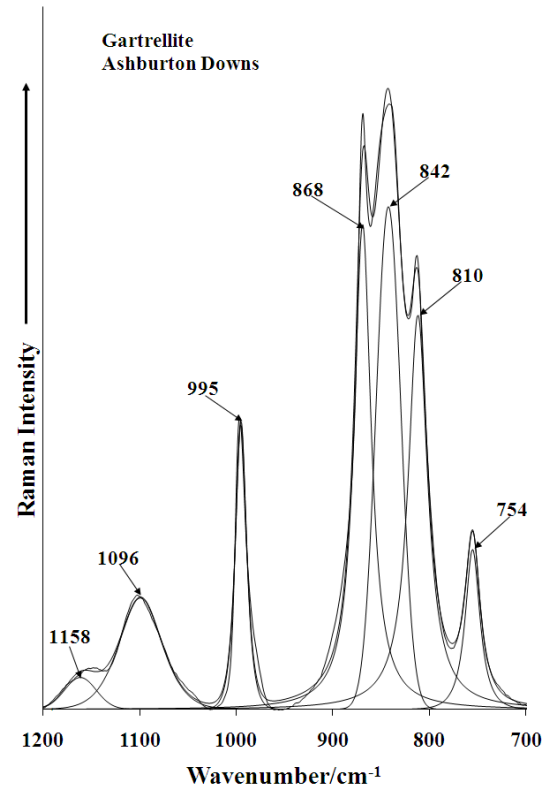
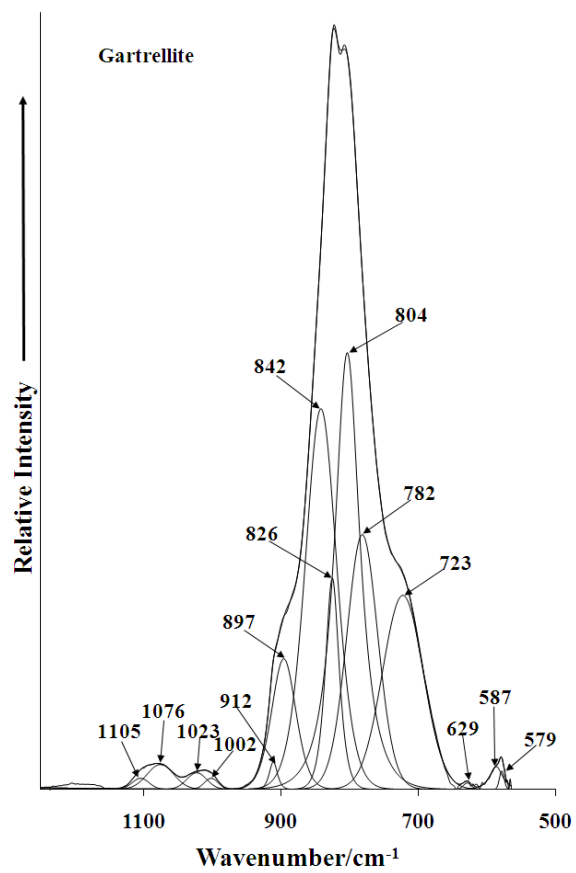


Figure 1b

281



282

283

284 **Figure 2**

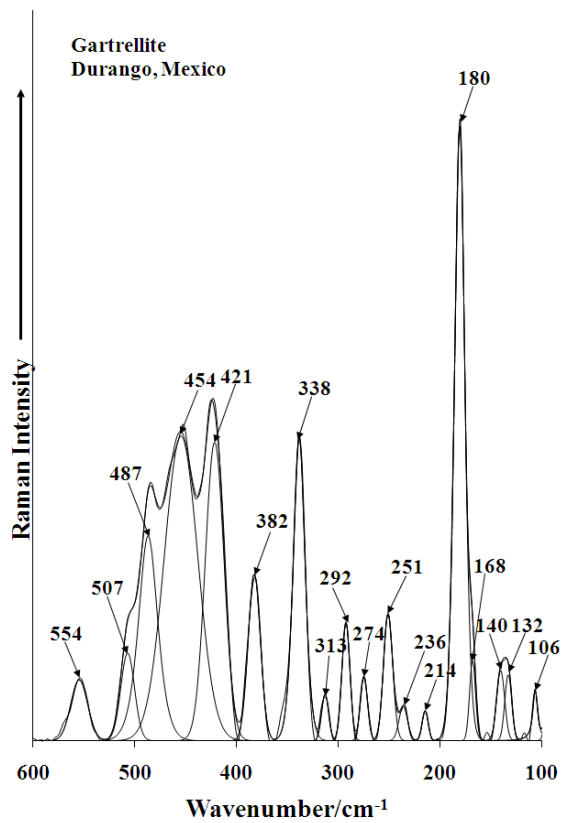


Figure 3a

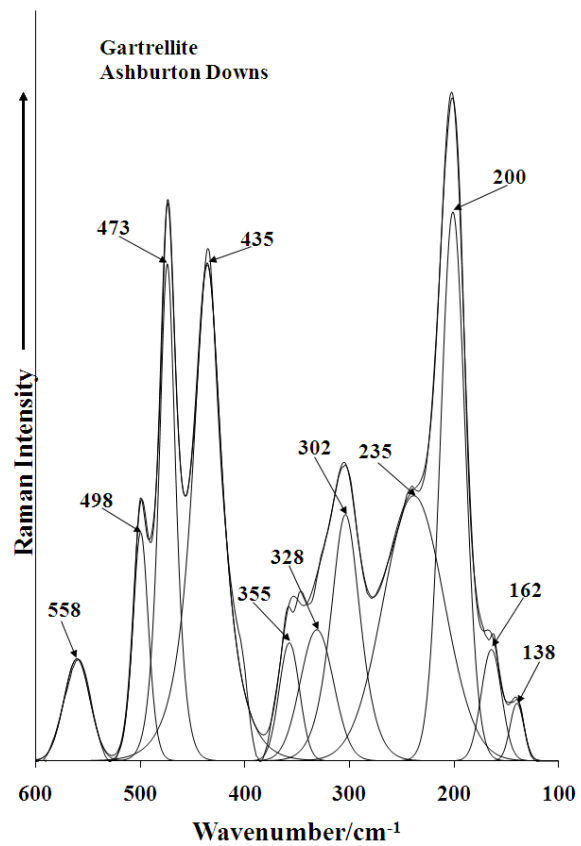


Figure 3b

286

287

288

289

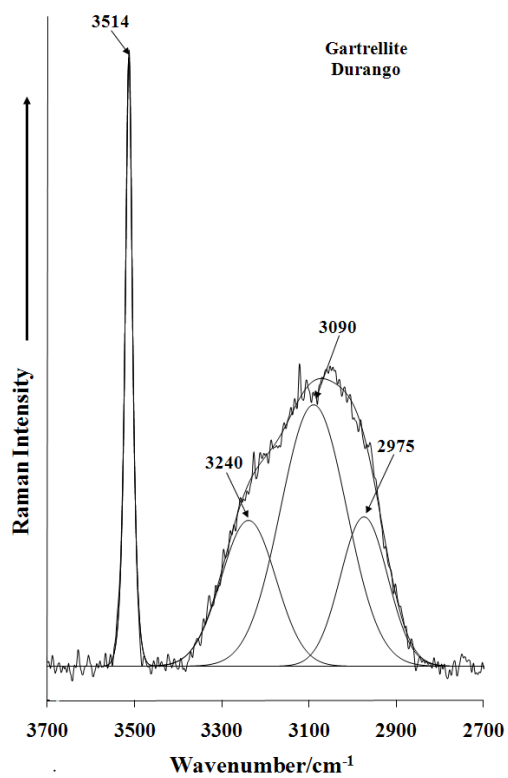


Figure 4a

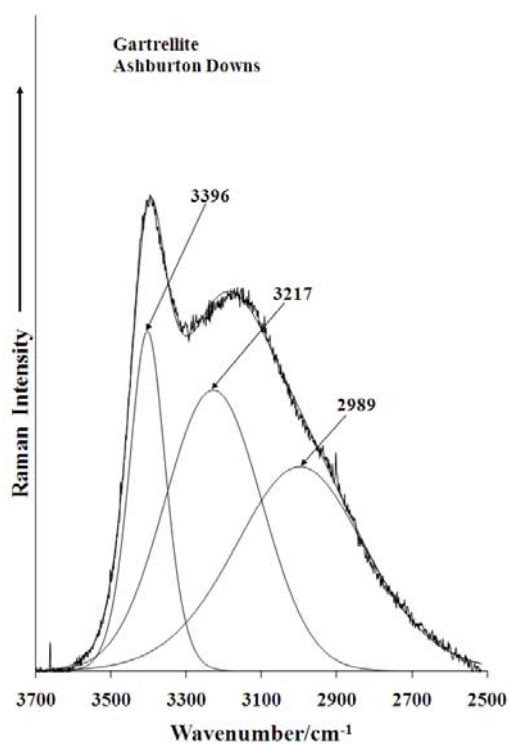


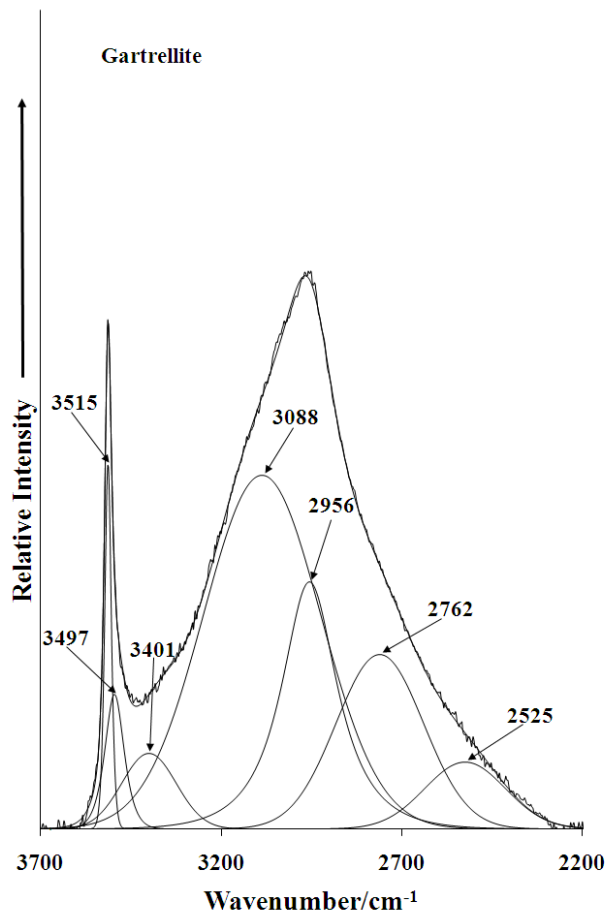
Figure 4b

291

292

293

294



295

296

297 **Figure 5**

298

299

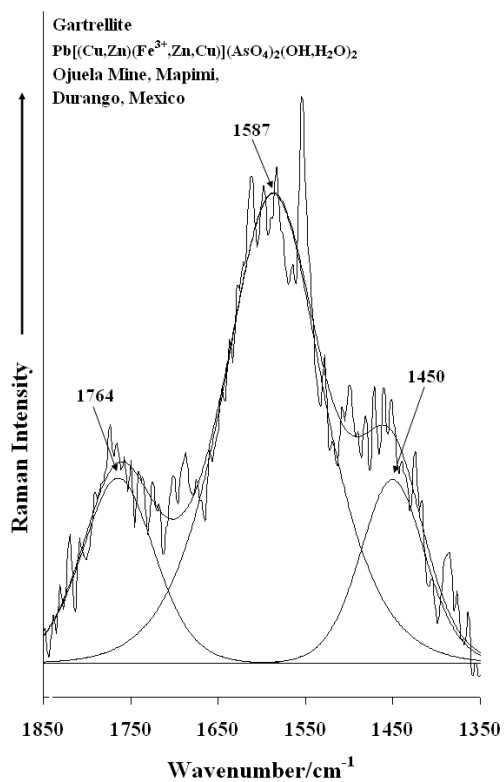


Figure 6a

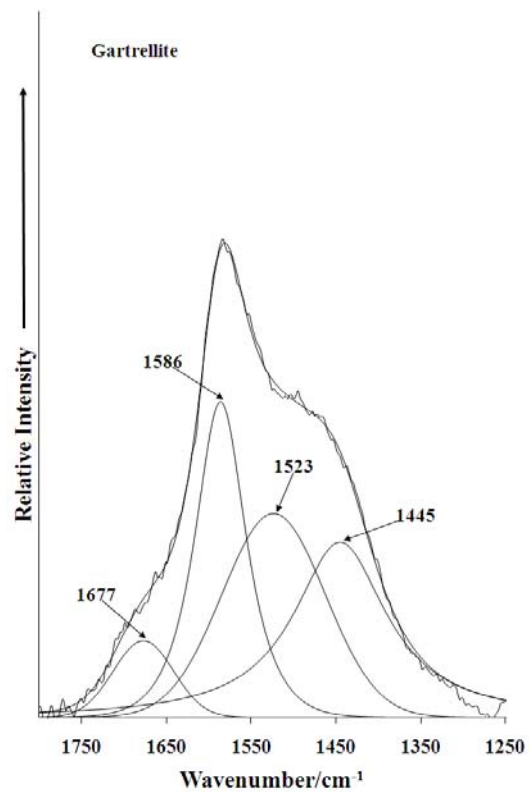


Figure 6b

301

302

303

304

305